Received: 14 June 2022 | Revised: 29 July 2022 | Accepted: 30 July 2022 | Published on: 12 August 2022

DOI: 10.1002/joc.7826

RESEARCH ARTICLE

International Journal of Climatology RMetS

Modelling wind speed across Zambia: Implications for wind energy

Brigadier Libanda | **Heiko Paeth**

Department of Physical Geography, Institute of Geography and Geology, University of Wuerzburg, Wuerzburg, Germany

Correspondence
Brigadier Libanda, Department of Physical Geography, Institute of Geography and Geology, University of Wuerzburg, Wuerzburg, Germany.
Email: brigadier.libanda@uni-wuerzburg.de

Funding information
Alexander von Humboldt-Stiftung

Abstract

Wind energy is a key option in global dialogues about climate change mitigation. Here, we combined observations from surface wind stations, reanalysis datasets, and state-of-the-art regional climate models from the Coordinated Regional Climate Downscaling Experiment (CORDEX Africa) to study the current and future wind energy potential in Zambia. We found that winds are dominated by southeasterlies and are rarely strong with an average speed of 2.8 $m \cdot s^{-1}$. When we converted the observed surface wind speed to a turbine hub height of 100 m, we found a ~38% increase in mean wind speed for the period 1981–2000. Further, both simulated and observed wind speed data show statistically significant increments across much of the country. The only areas that divert from this upward trend of wind speeds are the low land terrains of the Eastern Province bordering Malawi. Examining projections of wind power density (WPD), we found that although wind speed is increasing, it is still generally too weak to support large-scale wind power generation. We found a meagre projected annual average WPD of 46.6 $W \cdot m^{-2}$. The highest WPDs of ~80 $W \cdot m^{-2}$ are projected in the northern and central parts of the country while the lowest are to be expected along the Luangwa valley in agreement with wind speed simulations. On average, Zambia is expected to experience minor WPD increments of 0.004 $W \cdot m^{-2}$ per year from 2031 to 2050. We conclude that small-scale wind turbines that accommodate cut-in wind speeds of 3.8 $m \cdot s^{-1}$ are the most suitable for power generation in Zambia. Further, given the limitations of small wind turbines, they are best suited for rural and suburban areas of the country where obstructions are few, thus making them ideal for complementing the government of the Republic of Zambia's rural electrification efforts.

KEYWORDS

CORDEX Africa, renewable energy, wind speed, Zambia

1 | INTRODUCTION

While there is general scholarly unanimity that the climate needs protection, controversies about effective climate change mitigation strategies have raged unabated for a long time now. Several divergent accounts have been proposed, resulting in numerous controversies (Ginzky *et al.*, 2011; Rosenbloom *et al.*, 2020). However, one aspect on which

consensus seems to be established is that renewable energy is vitally important in the fight against climate change. It is projected that renewable energy will account for ~80% of the global electricity supply by 2050 compared to the current 26.2% (Hafner *et al*., 2018). This will drastically reduce carbon emissions thereby acting as a climate change mitigation pathway. Based on these estimations, a global shift toward a sustainable renewable energy future has been widely heralded with interest groups contending that it makes sense in both economic and climate mitigation terms (Turner, 1999; International Renewable Energy Agency, 2017).

Although the importance of renewable energy is well established, studies focusing on this crucial area of scientific enquiry, especially across southern Africa, are still limited. This limitation is particularly concerning because lack of access to energy represents one of the region's greatest impediments to socio-economic development (Penar, 2016; Sarkodie and Adams, 2020). It is estimated that an average person living in southern Africa consumes a meagre 200 kWh·year^{-1} compared to 9,086 kWh in high-income countries (Hafner *et al*., 2018). With populations projected to double in Africa by 2050 (UNFPA, 2010), any prospects of economic expansion across the region will require increased access to energy. The mainstay of any modern economy is reliable access to stable electricity especially as countries transition into digitally empowered societies (World Bank, 2019). Therefore, any southern African country that aims to transform its economy must address the issue of electricity head-on. It is important to note that pursuits to increase access to energy across the region must be within the realms of renewables if the global climate protection agenda is to be realized.

The growth of wind power is an example of renewables and represents one of the most well-known renewable technologies. The science underlying wind power generation is heavily rooted in climatic and allied sciences. It is now well understood that wind is triggered by nonuniform heating of the atmosphere by the sun (Ramudu and Alla, 2018), topographical variations including surface friction (Rueda *et al*., 2005), presence of water bodies or vegetation (Oyedepo *et al*., 2012), and rotation of the earth on its axis (Zaharim *et al*., 2008). The kinetic energy in wind is converted to electricity by wind turbines. The amount of energy a turbine can harvest is determined by wind speed, swept area, and the density of the air (Wood, 2011). It follows that for effective investment in wind energy, studies focussing on wind speed, swept area, and air density are pivotal.

Climate studies that investigate the spatiotemporal distribution of wind speed are increasingly used to inform the installation of both onshore and offshore wind turbines (Band *et al*., 2021; Ogunjobi *et al*., 2022). These studies are particularly important considering that climate variability triggers changes in wind speed and these should be thoroughly considered before establishing wind farms (Schaeffer *et al*., 2012; Band *et al*., 2021). Therefore, future wind speed variations need to be studied to understand the effect climate change exerts on wind energy potential across areas of interest especially considering that the effect of climate change on wind speed differs markedly from place to place (Davy *et al*., 2018).

Projections of wind speed are heavily dependent on coupled general circulation models (GCMs). The global nature of these models impedes the capturing of fine-scale wind speed variations (Randall *et al*., 2007). This challenge has been addressed by statistical and dynamical downscaling approaches (Najac *et al*., 2011; Reyers *et al*., 2014). Advances in downscaling GCMs include those of the Coordinated Regional Climate Downscaling Experiment (CORDEX), an internationally coordinated modelling attempt based on regional climate models. CORDEX models have been used in many studies and form the mainstay of the present study (see section 2.2.3) (Moemken *et al*., 2018; Li *et al*., 2020).

While variables such as wind speed, swept area, and air density are pivotal to wind energy generation, their assessment across southern Africa, particularly in Zambia, has been ignored. A lack of literature on future spatiotemporal variations of wind speed is especially apparent. The overarching goal of this study is to provide the first comprehensive assessment of wind speed projections across Zambia using the latest version of high-resolution CORDEX-Africa models. To satisfy the goal of this study, we address one important yet presently poorly understood research question: How will future wind speed vary at temporal and spatial scales across Zambia and what are the potential implications for wind energy generation?

2 | DATA SOURCES AND METHODOLOGY

2.1 | Study area

This study covers the whole of Zambia, a southern African country within the confines of longitudes 21°–34°E and latitudes 17.4°S and 7.6°S (Figure 1). Zambia is surrounded by several countries including the Democratic Republic of the Congo to the north, Tanzania to the northeast, Malawi and Mozambique to the east, Zimbabwe, Botswana, and Namibia to the south and Angola to the west.

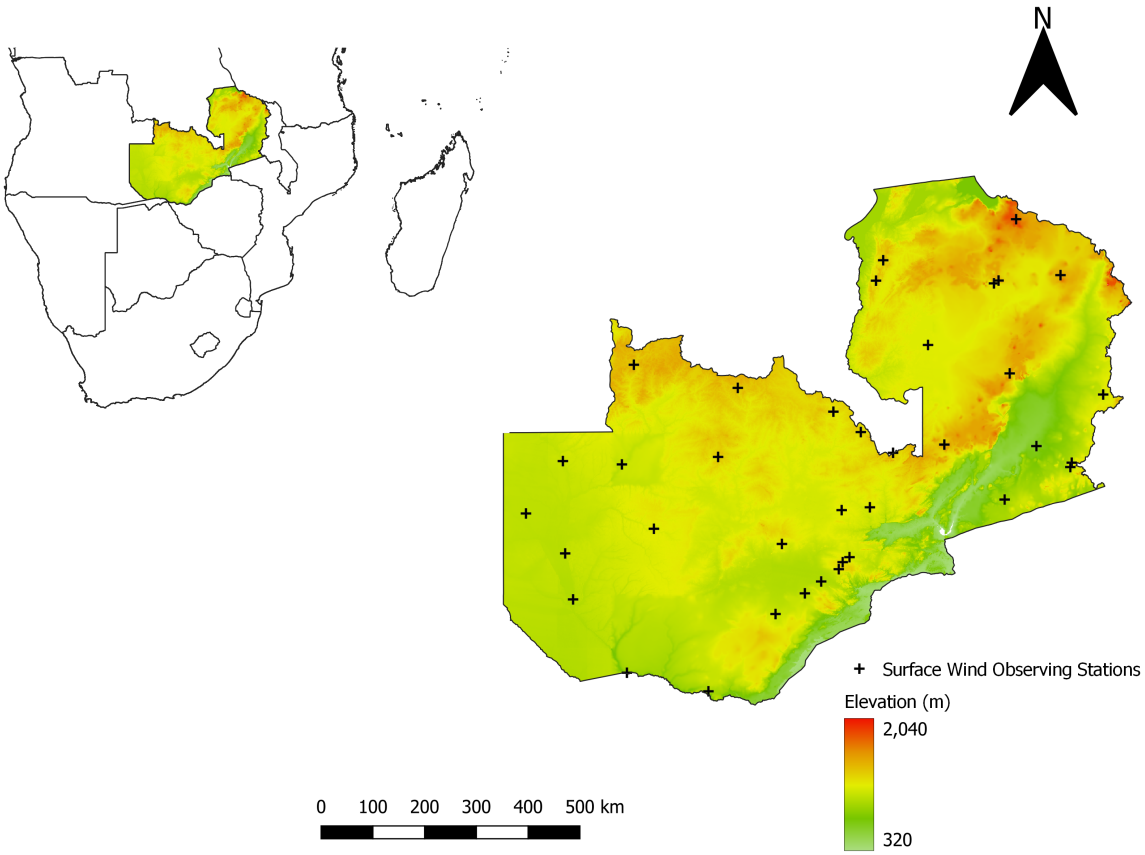

FIGURE 1 Map of the study area showing the spatial distribution of surface wind observing stations used in this study. The topographical data was retrieved from the archives of the Joint Institute for the Study of the Atmosphere and Ocean (JISAO; http://jisao.washington.edu; accessed April 1, 2022). It is a 1° × 1° latitude–longitude resolution elevation dataset. The inset shows the location of Zambia in southern Africa [Colour figure can be viewed at wileyonlinelibrary.com]

Although Zambia is described as a plateau with much of its landmass falling between 910 and 1,370 m above sea level, topographical variations are still apparent (Haberyan, 2018). For instance, the country's Muchinga escarpment in the Central Province is estimated to be higher than 1,800 m while parts of the Eastern Province especially in the valley of the Luangwa River, lie below 500 m. The topographical variations contribute to the modulation of wind speed across the country. In general, topography is known to alter the speed and trajectory of wind on both vertical and horizontal planes (Tse *et al*., 2020).

2.2 | Data sources

2.2.1 | Surface wind observing stations

Data from 37 surface wind observing stations across Zambia covering the period 2006–2021 measured at 10 m height was obtained from Ogimet (www.ogimet.com, accessed April 1, 2022) (Figure 1 and Table 1). Ogimet is a weather information service that archives surface synoptic observations (Synops), METeorological Aerodrome Reports (METARs), and Terminal Aerodrome Forecasts (TAFs) from around the world in near real-time. The data for Zambia are available at hourly intervals. All the surface wind observing stations use cup counter anemometers installed as specified in the Guide to Global Observation Systems of the United Nations World Meteorological Organization (WMO, 2013).

We used the *climate* package (Czernecki *et al*., 2020) in R Programming Language (R Core Team, 2020) to automatise the decoding and downloading of data from Ogimet. We then subjected the downloaded data to quality control checks which involved the removal of strangely large or small values. For example, based on expert knowledge from the study area (Munyeme and Jain, 1994; Kanno *et al*., 2013), all wind speed data ≥30 knots, representing ∼3% of the full dataset, were removed. Further, all negative entries representing 0.1% of the full dataset were also removed. As the removed values are generally unexpected in the study area, we thought of them as being a result of human error. In the

TABLE 1 Detailed information for surface wind observing stations used in this study showing World Meteorological Organization (WMO) station identifiers, station names, latitude, longitude, and elevation

WMO No.	Station	Latitude	Longitude	Elevation
67581	Chipata Met	−13.564	32.589	1,025
67753	Choma Agro Met	−16.383	27.07	1,275
67543	Kabompo Met	−13.596	24.208	1,090
67662	Kabwe Agro Met	−14.395	28.828	1,175
67663	Kabwe Met	−14.448	28.302	1,204
67563	Kafironda Agro Met	−12.614	28.148	1,220
67659	Kafue Polder Met	−15.777	27.921	976
67641	Kaoma Agro Met	−14.795	24.804	1,158
67475	Kasama Airport Met	−10.224	31.14	1,384
67541	Kasempa Met	−13.457	26	1,334
67403	Kawambwa Met	−9.793	29.076	1,334
67743	Livingstone Int Airport Met	−17.823	25.82	991
67583	Lundazi Agro Met	−12.294	33.175	1,138
67666	Lusaka City Airport Met	−15.417	28.321	1,274
67665	Lusaka Int Airport Met	−15.324	28.448	1,153
67751	Magoye Agro Met	−15.998	27.617	1,025
67461	Mansa Airport Met	−10.173	28.942	1,257
67413	Mbala Met	−9.028	31.553	1,665
67599	Mfuwe Met	−13.255	31.931	557
67476	Misamfu Agro Met	−10.171	31.225	1,378
67633	Mongu Met	−15.254	23.151	1,048
67477	Mpika Met	−11.901	31.433	1,399
67580	Msekera Met	−13.646	32.563	1,011
67667	Mt. Makulu Agro Met	−15.548	28.248	1,221
67655	Mumbwa Airport Met	−15.078	27.189	1,209
67441	Mwinilunga Met	−11.74	24.431	1,365
67561	Ndola Int Airport Met	−12.994	28.659	1,269
67673	Petauke Met	−14.251	31.339	1,022
67469	Samfya Marine Met	−11.371	29.911	1,194
67731	Senanga Agro Met	−16.111	23.298	1,012
67571	Serenje Agro Met	−13.227	30.215	1,390
67741	Sesheke Agro Met	−17.477	24.301	942
67551	Solwezi Airport Met	−12.171	26.367	1,384
67531	Zambezi Met	−13.534	23.108	1,065
67481	Isoka Met	−10.07	32.38	1,360
67575	Mkushi Agro Met	−13.38	29.26	1,237
67625	Kalabo Agro Met	−14.51	22.42	1,033

final step of the station data preparation, we converted all wind speed data from knots to $m \cdot s^{-1}$ to conform to the widely used International System of Units in wind energy studies. Considering that only 3.1% of the data was discarded, the final dataset was regarded as high quality.

While wind power fluctuates on various time scales such as daily and subdaily (Moemken *et al.*, 2018; Weber *et al.*, 2018), we mainly focus on monthly and annual fluctuations in this study because wind turbines need to be in areas with a lot of wind on a regular basis, which is more important than having occasional high winds. Further, our exploratory analyses showed that wind speed for hourly, daily, monthly, and annual timescales fall within the same range across Zambia, and this is consistent with

previous research in the study area (Munyeme and Jain, 1994; Kanno *et al.*, 2013).

2.2.2 | Gridded datasets

Since surface wind observing station data only covers the period 2006–2021, we retrieved two gridded datasets and examined their ability to reproduce surface wind observing station data. The comparative methods employed herein involved the use of gridded datasets for only the grid cells containing cup counter anemometers. The best-performing dataset is finally used for subsequent analyses.

The first dataset we retrieved is TerraClimate, a 4-km high-resolution monthly climate dataset archiving several variables such as temperature, precipitation, vapour pressure, solar radiation, wind speed, and so forth covering the period 1958 to the near-present (Abatzoglou *et al.*, 2018). TerraClimate was developed by combining climate normals from WorldClim version 1.4 and version 2 datasets (Fick and Hijmans, 2017), the Climatic Research Unit Timeseries version 4.0 (Harris *et al.*, 2014), and JRA-55 (Ebita *et al.*, 2011). TerraClimate data are widely used in applied climate studies (e.g., Abdi, 2019).

The other dataset we evaluated is ERA5, the fifth-generation global climate reanalysis developed and maintained by the European Centre for Medium-Range Weather Forecasts. The dataset has a $0.25° \times 0.25°$ horizontal resolution and covers the period 1979 to near present at a height of 10 m. ERA5 was developed by assimilating observations in a global weather forecast model (Hersbach *et al.*, 2020).

2.2.3 | Regional climate models

We used regional climate models (RCMs) driven by GCMs from the Coordinated Regional Climate Downscaling Experiment (CORDEX Africa 0.44; Giorgi *et al.*, 2009) to study the future wind energy potential in Zambia under an intermediate and a business-as-usual emission scenario (representative concentration pathway; RCP4.5 and RCP8.5 respectfully; see Table 2). The RCP4.5 is a stabilization scenario that keeps radiative forcing at 4.5 $W \cdot m^{-2}$. This pathway was updated from earlier versions of the Global Change Assessment Model by including retrospective emissions and land cover data; RCP4.5 can be considered a cost-minimizing pathway (Thomson *et al.*, 2011). The RCP8.5 is a high-emissions scenario which gives the likely outcome when no determined efforts are made to cut GHG emissions (Riahi *et al.*, 2011).

2.3 | Methodological approach

2.3.1 | Measures of reliability and the climatological normal

We used the Taylor diagram to find a suitable gridded dataset to be used in subsequent analyses in place of surface wind observations. Taylor diagrams are useful in gauging the relative skill of multiple datasets as they include root mean square errors, correlation coefficient (R), and standard deviation all at once (Taylor, 2001).

We further used R and percent bias (PBias; Gupta *et al.*, 1999) to assess the reliability of models and choose those to be included in the ensemble which was developed using climate data operators (CDO; Schulzweida, 2021). PBias is a convenient way of assessing the skill of models because results are given in percentage. It thus shows the positive or negative behaviour of models with regards to observational data in percentage. Models showing performance of <50% and as close enough to zero are generally regarded as well-performing (Moriasi *et al.*, 2007). We also compared trends which we calculated using the modified Mann–Kendall test for serially correlated data as suggested in the Hamed and Rao (1998) variance correction approach.

Climatological normals, typically covering 30 years, are used in climate change studies as a standard reference period. The most recent WMO recommended period is 1981–2010. Unlike the 1961–1990 baseline which was until recently widely used, the 1981–2010 period includes key observations from satellites that aid research activities. In this study, we use a 20-year reference period (i.e., 1981–2000) to account for historical simulations of RCMs that do not cover the full 1981–2010 period (WMO, 2017). The 1981–2000 reference period has previously been used as a baseline to assess wind power potential in the Gulf of Oman (Band *et al.*, 2021) and to study potential climate change and afforestation effects on wind power in the western African country of Nigeria (Matthew and Ohunakin, 2022).

2.3.2 | Bias correction

Having observed some biases in model outputs, we used linear scaling (LS), a bias-correction technique that is widely used in modelling studies to adjust model outputs (Ines and Hansen, 2006; Teutschbein and Seibert, 2012; Shrestha *et al.*, 2017). In a nutshell, LS considers the difference between mean station data and model outputs and then applies it to the outputs. The Shrestha (2015) software was used for this analysis.

TABLE 2 Overview of the global and regional climate models used in this study

Driving GCM	RIP	RCM	Scenario	Period	Resolution
CanESM2	r1i1p1	RCA4	Historical	1981–2000	0.44° × 0.44°
IPSL-CM5A-MR	r1i1p1	RCA4	Historical and future	1981–2100	0.44° × 0.44°
CNRM-CM5	r1i1p1	RCA4	Historical	1981–2000	0.44° × 0.44°
CSIRO-MK3.6.0	r1i1p1	RCA4	Historical	1981–2000	0.44° × 0.44°
EC-EARTH	r1i1p1	RCA4	Historical	1981–2000	0.44° × 0.44°
MPI-ESM-LR	r1i1p1	RCA4	Historical	1981–2000	0.44° × 0.44°
GFDL-ESM2M	r1i1p1	RCA4	Historical and future	1981–2100	0.44° × 0.44°
HadGEM2-ES	r1i1p1	RCA4	Historical and future	1981–2100	0.44° × 0.44°
MIROC5	r1i1p1	RCA4	Historical	1981–2000	0.44° × 0.44°
NorESM1-M	r1i1p1	RCA4	Historical	1981–2000	0.44° × 0.44°
HadGEM2-ES	r1i1p1	RegCM4	Historical	1981–2000	0.44° × 0.44°
MPI-ESM-MR	r1i1p1	RegCM4	Historical	1981–2000	0.44° × 0.44°

Note: Models used for future analyses are slanted. The models used are the ones that were available at the time of analyses here: https://climate4impact.eu/impactportal/general/index.jsp.
Abbreviations: GCM, general circulation model; RCM, regional climate model; RIP, index of the considered ensemble member.

2.3.3 | Wind energy potentials

Wind power generation is very dependent on the wind speed available at the hub height. In the present study, we use the term hub height to refer to the distance from the platform to the rotor of a wind turbine—in this case, 100 m. However, the 100 m we consider here is much higher than the 10 m height provided by ERA5. Therefore, we converted ERA5 wind speed at height h to the turbine height z using the power law (Brown *et al.*, 1984; Kubik *et al.*, 2013),

$$V_z = V_h \left(\frac{z}{h}\right)^{\alpha}, \tag{1}$$

where V_z denotes the wind speed at height z and V_h denotes the wind speed at height h. α is the wind shear coefficient which heavily depends on the stability of the atmosphere and tends to be higher in a stable and stratified atmosphere with high surface roughness (Jung and Schindler, 2021; Ogunjobi *et al.*, 2022). By extension, α changes with variations in vegetation cover, wind speed, elevation, temperature, and other atmospheric variables (Kikumoto *et al.*, 2017). In the present study, we applied the power exponent of 0.14 as it is considered appropriate for open land surfaces (Storm *et al.*, 2009; Akinsanola *et al.*, 2017; Sawadogo *et al.*, 2019). Further, considering the tropical climate of Zambia, upper atmospheric conditions such as rapid changes in temperature and icing have a near-zero effect on the conversion of h to z; therefore, we did not factor this in our conversion. Many studies in warm climates found upper atmospheric conditions to have negligible effects (Davy *et al.*, 2018; Band *et al.*, 2021).

To assess the amount of energy available across Zambia, we used wind power density (WPD; $W \cdot m^{-2}$), a widely used physical transformation in wind energy studies (Band *et al.*, 2021; Ogunjobi *et al.*, 2022). WPD can be thought of as the amount of kinetic energy from the wind per unit area that can be harnessed into energy production (Hennessey Jr, 1977),

$$\mathrm{WPD} = \frac{1}{2}\left(\rho V^3\right), \tag{2}$$

where ρ is the air density in $kg \cdot m^{-3}$ and V is the mean wind speed in $m \cdot s^{-1}$.

3 | RESULTS AND DISCUSSION

3.1 | Near-surface wind climatology

In situ climate observations at the 10 m height indicate that Zambia is dominated by southeastern near-surface winds at an average speed of 2.8 $m \cdot s^{-1}$ (Figure 2a). While there are variations from season to season, results show that southeasterlies remain dominant throughout the year. Minor differences are observed during the December–February (DJF) season when southwesterlies prevail (Figure 2b). During the March–May (MAM; Figure 2c) and June–August (JJA; Figure 2d) seasons, the winds turn back to southeasterlies before veering again from September–November (SON; Figure 2e).

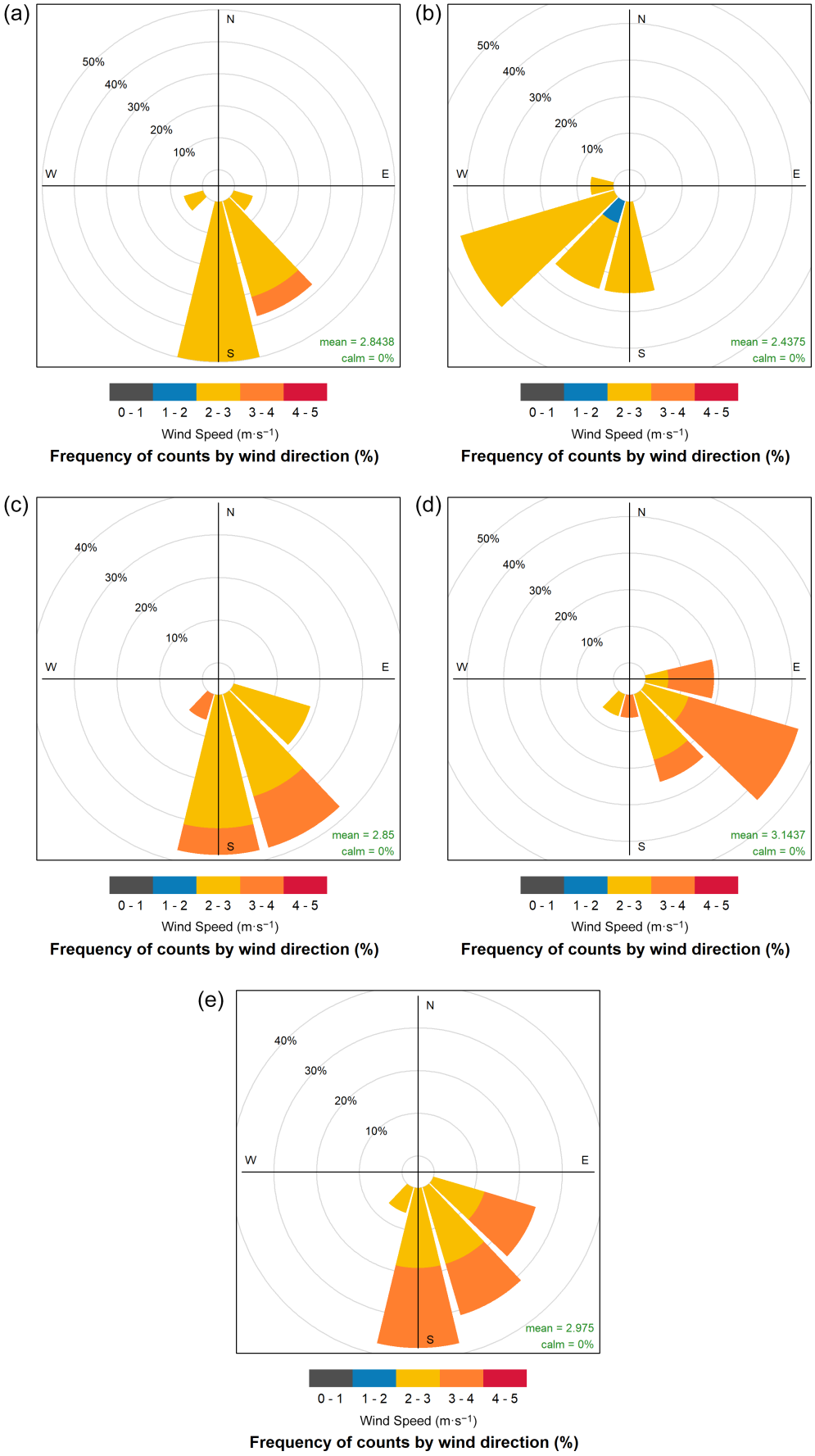

FIGURE 2 Frequency distribution of wind speed and direction for (a) annual average; (b) DJF season; (c) MAM season; (d) JJA season; and (e) SON season based on data from surface wind observing stations for the period 2006–2021 [Colour figure can be viewed at wileyonlinelibrary.com]

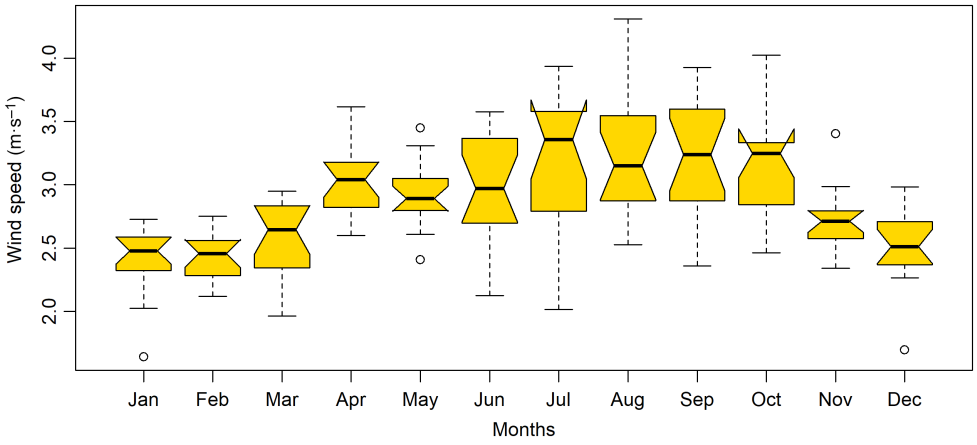

FIGURE 3 Month-to-month variations of wind speed across Zambia based on data from surface wind observing stations for the period 2006–2021. The lower horizontal line of each boxplot represents the first quartile (Q1), that is, the middle number between the smallest and the median of the wind speed dataset. The yellow part represents the interquartile range (IQR), that is, 25th to the 75th percentile. The horizontal line in the IQR represents the median of the dataset. The upper horizontal line shows the Q3. All datasets shown outside the boxplots are outliers [Colour figure can be viewed at wileyonlinelibrary.com]

The observed climatological southeasterly wind system is responsible for moisture advection from the Indian Ocean and the tropical South Atlantic Ocean, thus contributing significantly to the rainfall patterns in Zambia and across the region (Hachigonta and Reason, 2006). While there are variations in wind speed from season to season, the observed 2.8 $m{\cdot}s^{-1}$ mean wind speed has undergone a 12% increase since 1994 (Munyeme and Jain, 1994). The seasonal variations in wind speed can be attributed to atmospheric kinetics that are driven by changes in solar radiation from season to season (Zhou *et al.*, 2021).

Results further indicate that with average near-surface wind speeds of 2.8 $m{\cdot}s^{-1}$, a minimum of 1.6 $m{\cdot}s^{-1}$, and a maximum of 4.3 $m{\cdot}s^{-1}$, winds are rarely strong in Zambia (Figure 3). The maximum wind speed was observed in August while the minimum was reported in January. It is notable however that calm conditions are generally nonexistent across the country, and this can be attributed to the subtropical climate with prevailing trade winds within the Hadley circulation (Del Genio, 1997; Freychet *et al.*, 2021).

The observed mean average mean wind speed of 2.8 $m{\cdot}s^{-1}$ is consistent with wind speeds reported in neighbouring Malawi (Ngongondo *et al.*, 2012) and nearby South Africa (Shonhiwa, 2015) but is slower than those reported in the Mediterranean climate of Morocco where they reach up to 9.04 $m{\cdot}s^{-1}$ (El Khchine *et al.*, 2019).

3.2 | Measures of reliability

Since station-based data only covers the period 2006 to near-present, we examined the ability of ERA5 and TerraClimate to reproduce station data with the aim of using the one with better performance in subsequent analyses. Both datasets were found to perform relatively well (Figure 4) suggesting that the use of either of them would yield very similar results. However, with a correlation coefficient (R) of 0.6, a root mean square error (RMSE) of only 0.14 ($m{\cdot}s^{-1}$), and a standard deviation of <0.05, ERA5 exhibits slightly better performance (Figure 4).

The good performance of ERA5 is not surprising and it has been used in place of station data in many data-scarce regions. For instance, ERA5 was found useful in the projection of wind energy potential over West Africa (Akinsanola *et al.*, 2021), it was used in a combined wind-solar electricity production potential over northwestern Africa (Jánosi *et al.*, 2021), and most recently, it was used to compare the wind energy potential at 120 and 140 m hub height (Jung and Schindler, 2022). Based on these findings, ERA5 was used in subsequent analyses of the present study in place of station data.

A cursory review of regional climate models (RCMs) in simulating retrospective wind speed across the study area indicated that with biases of <24%, RCA4_HadGEM2-ES, RCA4_IPSL-CM5A-MR, RCA4_GFDL-ESM2M performed better than all other models. These biases translate into ~0.6 $m{\cdot}s^{-1}$, thus suggesting that the models perform very well compared to other places such as West Africa where RCMs were found to have biases of 2.2 $m{\cdot}s^{-1}$ (Ogunjobi *et al.*, 2022). Further, with correlation coefficients ranging between 0.4 and 0.7 during the reference period (1981–2000), these models were found to have the strongest positive relationship with ERA5 (Figure 5).

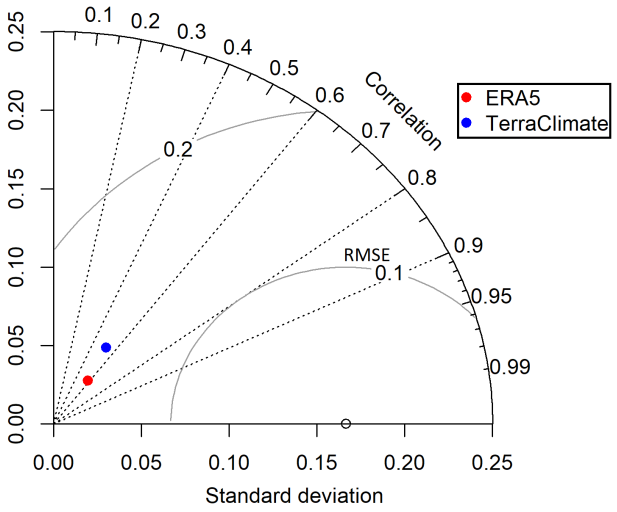

FIGURE 4 Statistical comparison between wind speed ($m \cdot s^{-1}$) station data and estimates of ERA5 and TerraClimate across Zambia for the period 2006–2021, using a Taylor diagram [Colour figure can be viewed at wileyonlinelibrary.com]

Concerning the long-term changes over the 1981–2000 period, it is notable that 58.3% of the models have an inverse relationship with ERA5 (Figure 5). This contrary relationship suggests that when wind speed increases (decreases) across Zambia, the following models simulate a reduction (increase): RegCM4_HadGEM2-ES ($R = -0.3$), RCA4_NorESM1-M ($R = -0.2$), RegCM4_MPI-ESM-MR ($R = -0.4$), RCA4_MPI-ESM-LR ($R = -0.2$), RCA4_CNRM-CM5 ($R = -0.2$), and RCA4_MIROC5 ($R = -0.6$). In general, models that mimic past climate well are preferred because they inherently simulate future climate features well (Lovino *et al.*, 2018).

Considering the relatively good performance of RCA4_-HadGEM2-ES, RCA4_IPSL-CM5A-MR, and RCA4_GFDL-ESM2M, we created an ensemble of these models and examined its performance. We noticed that with a correlation coefficient of 0.68, the ensemble improved significantly (Figure 5). The improvement in the performance of the ensemble was not surprising as their use is widely recommended because they tend to have better predictive performance (Sillmann *et al.*, 2013). In a nutshell, individual models tend to have biases inherent in their initialization and parameterization schemes and ensembles help to reduce these biases (Reyers *et al.*, 2016; Ogunjobi *et al.*, 2022). We, therefore, used the ensemble for further analyses.

3.3 | Wind speed extrapolation and future variations

When we converted ERA5 wind speed from 10 m to the hub height of 100 m, wind speeds increased considerably (Figure 6). Specifically, we observed a ~ 38% increase in mean wind speed from 2.5 $m \cdot s^{-1}$ at 10 m to 3.4 $m \cdot s^{-1}$ at 100 m. We also noted that the range increased from 1.6–3.5 $m \cdot s^{-1}$ at 10 m to 2.2–4.5 $m \cdot s^{-1}$ at 100 m.

High wind speeds at high levels are attributed to larger distances from frictional effects at the surface (Türk and Emeis, 2010; Liu *et al.*, 2019). Altogether, surface roughness is an important determinant of wind speed with implications on the aerodynamic performance of wind turbines. Further, air at the ground level is denser and decreases upwards. As such, any external force on the air will cause the wind to be faster at high altitudes than near the ground (Emeksiz and Cetin, 2019).

Both model and observed wind speed data show an increase in wind speed across Zambia (Figure 7). Results further indicate that wind speed increments were more pronounced from 1979 to 2021 (Slope = 0.002) than they are expected to be from 2022 to 2100 (RCP4.5 Slope = 1.64896e-4 and RCP8.5 slope = −9.9109e-5). This observation suggests that wind power potential has been increasing across the country. This upward tendency will continue until the end of the century but will likely be at a slower pace from 2022 to the middle of the century and thereafter very minimal under RCP4.5 and likely to reduce under RCP8.5. Further comparative analysis between RCP4.5 and RCP8.5 for the period 2022–2100 shows very minor differences (Figure 7). Specifically, both emission scenarios indicate that the trend of wind speed will be near stationary.

Spatially, the trend of wind speed was again found to be increasing across the whole country during the period 1979–2021 (Figure 8). The only area that shows slight reductions is the Kafue region and the Eastern Province bordering Malawi where slight wind speed decreases of 0.001 $m \cdot s^{-1}$ were experienced every year.

The observation that wind speed is increasing and is expected to continue rising is consistent with model projections elsewhere. For instance, since 2010, the mean global wind speed has increased from ~3.1 to ~3.3 $m \cdot s^{-1}$ thus, potentially increasing wind energy by ~17 ± 2% (Zeng *et al.*, 2019). In Africa, projections indicate that wind speed increments will potentially increase wind power density by ~70% (Akinsanola *et al.*, 2021). While these results are true for the continent, local differences should be expected. For instance, the Cape Region of South Africa has been experiencing an annual wind speed reduction of −0.002 $m \cdot s^{-1}$ (Wright and Grab, 2017). These differences underpin the need for localized wind speed studies and highlight deficiencies inherent in generalized or global studies; while useful in giving a general overview, global studies miss climate variations occurring at the local scale.

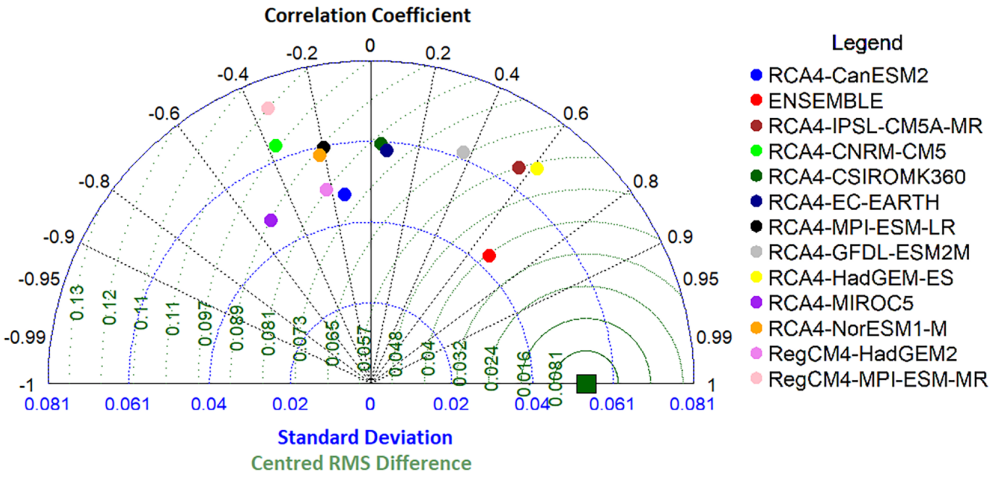

FIGURE 5 Relationships between regional climate models and ERA5 in simulating annual wind speed across Zambia (averaged across longitude 21°–34°E and latitude 17.4°S and 7.6°S) during the reference period, 1981–2000 [Colour figure can be viewed at wileyonlinelibrary.com]

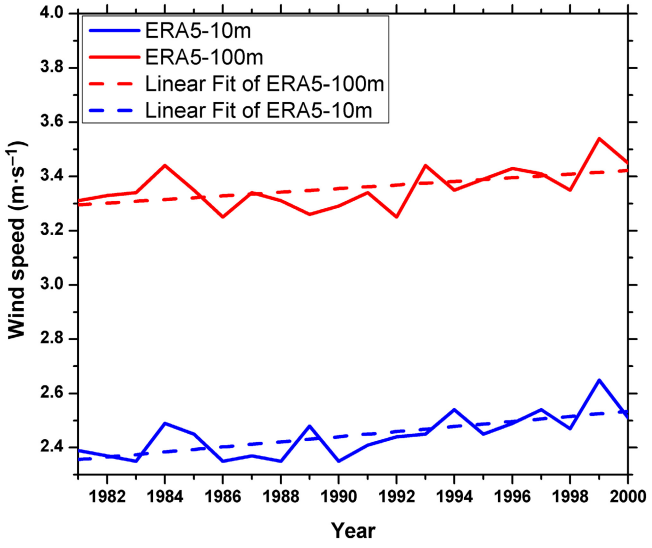

FIGURE 6 Time series of average wind speed (m·s^{-1}) across Zambia (averaged across longitude 21°–34°E and latitude 17.4°S and 7.6°S) measured at 10 m height and conversion to 100 m hub height, based on ERA5 [Colour figure can be viewed at wileyonlinelibrary.com]

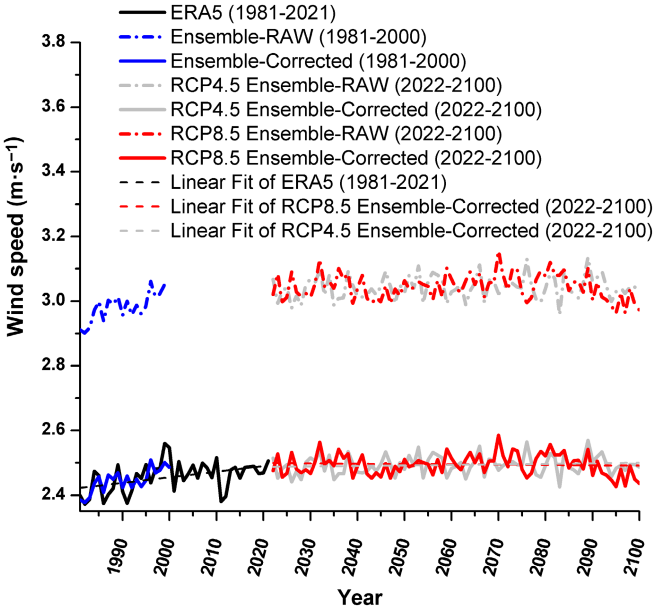

FIGURE 7 Trends in wind speed across Zambia for the period 1979–2100 based on ERA5 (slope = 0.002), ensemble historical raw, ensemble historical bias-corrected, RCP4.5 future raw ensemble, RCP4.5 future bias-corrected ensemble (slope = 1.64896e-4), RCP8.5 future raw ensemble, RCP8.5 future bias-corrected ensemble (slope = −9.9109e-5). The bias correction was based on ERA5 for the period 1981–2000 [Colour figure can be viewed at wileyonlinelibrary.com]

Spatial analyses of projected wind speed anomalies until 2050 also reveal increments across much of the country (Figure 9). Most parts of the country are expected to experience wind speed increments ranging between 0 and 1 m·s^{-1} although it is notable that parts of northern Zambia covering Isoka, Kasama, Mbala, and Kaputa are projected to experience wind speed increments of up to 1.5 m·s^{-1} (Figure 9). The only areas that divert from this upward trend of wind speeds are the low land terrain of the Eastern Province bordering Malawi (see Figure 1). These parts of the country are projected to experience negative wind speed anomalies of up to 1 m·s^{-1}.

Slow wind speeds in parts of the Eastern Province can be attributed to the Luangwa Valley geometry, an extension of the Great East African Rift Valley. Valleys are known to be widely influenced by thermally driven winds which develop due to differences in heating of adjacent air masses, inhomogeneous land distribution generally induces slower winds in down-valley compared to up-valley areas (Wagner *et al.*, 2014).

Overall, no significant differences in spatial wind anomalies have been detected between RCP4.5 and RCP8.5 or between the middle (2031–2050) and end (2081–2100) of the century thus suggesting that wind

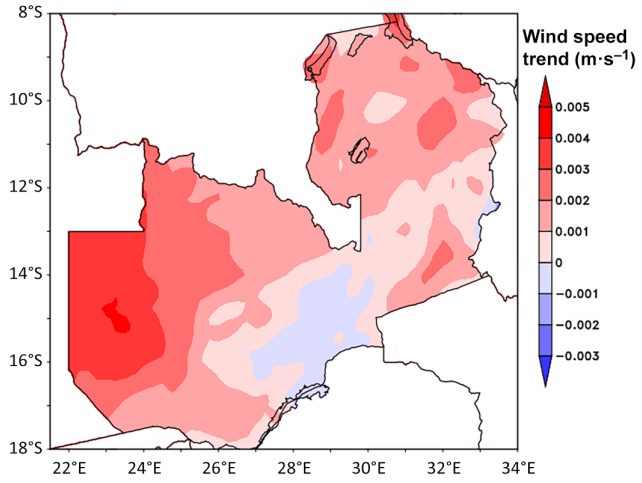

FIGURE 8 Spatial wind speed trends across Zambia for the period 1979–2021 based on ERA5. The wind speed was measured at the 10-m height [Colour figure can be viewed at wileyonlinelibrary.com]

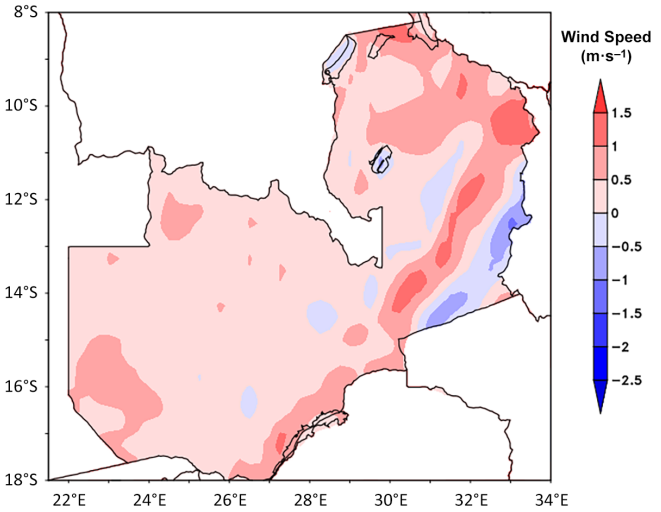

FIGURE 9 Wind speed anomalies ($m \cdot s^{-1}$) at the 100 m hub height for the mid-century (2031–2050) relative to the 1981–2000 baseline climate, using the RCP4.5 ensemble scenario. The end of the century (2081–2100) and RCP8.5 wind speed anomalies are similar to the above, therefore, they are not shown [Colour figure can be viewed at wileyonlinelibrary.com]

power potential is likely to be consistent until the close of the century.

3.4 | Future changes in wind power density across Zambia

Examining projections of wind power density (Figure 10), we found that although wind speed is increasing, it is still generally too weak to support large-scale wind power generation. We found the projected annual average wind power density (WPD) to be about 46.6 $W \cdot m^{-2}$. The highest WPDs of ~80 $W \cdot m^{-2}$ are projected in the northern and central parts of the country while the lowest are to be expected along the Luangwa valley in agreement with wind speed simulations (see Figure 9). Northwestern and Luapula provinces bordering the Democratic Republic of Congo are also projected to experience low WPDs ranging from ~40 to ~50 $W \cdot m^{-2}$.

Even considering the maximum projected WPDs of ~80 $W \cdot m^{-2}$, wind power resources are found to be generally weak as per National Renewable Energy Laboratory (NREL) classification (Table 3). These results suggest that only small-scale turbines can be supported in the Zambian setup. Depending on the model, some wind turbines accommodate cut-in wind speeds of 3.8 $m \cdot s^{-1}$ which can produce ~60,000 to slightly below 180,000 kWh annually (CoC, 2022). While small wind turbines have less generating capacity compared to commercial ones, this output is enough to power anywhere between 8 and 23 ordinary houses every year. Given the limitations of small wind turbines, they are best suited

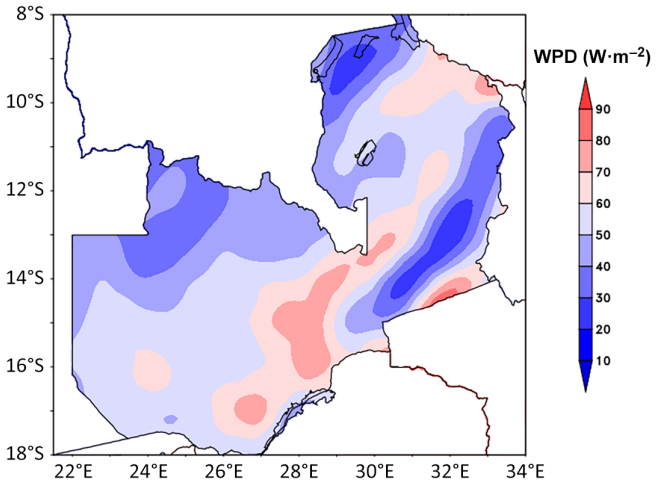

FIGURE 10 Anomalies of mean wind power density ($W \cdot m^{-2}$) at the 100 m hub height for the mid-century (2031–2050) relative to the 1981–2000 baseline climate, using the RCP4.5 ensemble scenario. The end of the century (2081–2100) and RCP8.5 wind speed anomalies are similar to the above, therefore, they are not shown [Colour figure can be viewed at wileyonlinelibrary.com]

for rural and suburban parts of Zambia where obstructions are few, thus making them ideal for complementing the government of the Republic of Zambia's rural electrification efforts (Haanyika, 2008). Commercial windpumps also appear viable and can supplement rainfed agriculture in dry seasons.

Considering the ~38% increase in wind speed when extrapolated from 10 to 100 m hub height (Figure 6),

TABLE 3 National Renewable Energy Laboratory wind power density classification (https://www.nrel.gov/; accessed May 10, 2022)

Wind power class	Wind power density ($W \cdot m^{-2}$)	Resource potential
1	0–200	Not suitable
2	200–300	Probable for standalone systems
3	300–400	Good
4	400–500	Good
5	500–600	Excellent
6	600–800	Outstanding
7	800–2,000	Superb

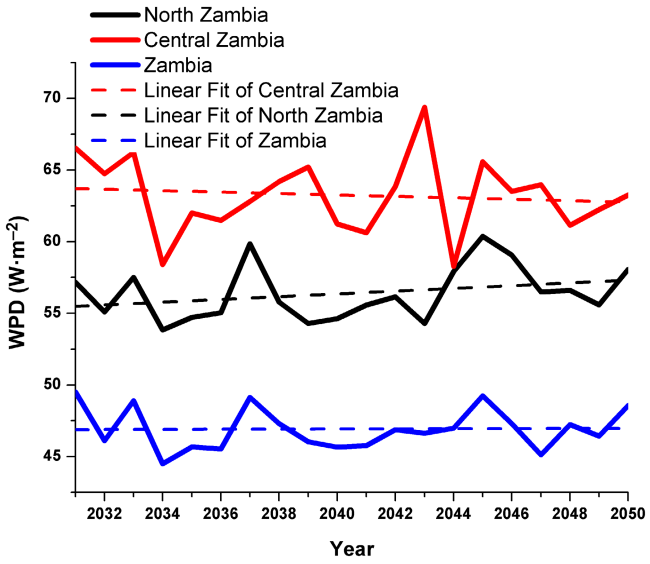

FIGURE 11 Time series of mean wind power density ($W \cdot m^{-2}$) at the 100 m hub height for the mid-century (2031–2050), using the RCP4.5 ensemble scenario. Central Zambia covers Lon 27°–29°E and Lat 17°–14°S while northern Zambia is over Lon 30°–33°E and Lat 11°–9°S. The blue curve represents the whole country [Colour figure can be viewed at wileyonlinelibrary.com]

ultra-tall wind turbines fitted with larger rotors would be necessary for large-scale wind power generation. Large turbine rotors with longer blades translate into better aerodynamic efficiency by covering more swept area which allows the capturing of more wind and thus more electricity production.

Although the wind energy potential is low along the Luangwa valley (Figure 10), other renewable energy sources such as leveraging the Luangwa River's hydropower potential remain possible. The Luangwa River is one of the biggest unaltered rivers in the southern African region and remains the biggest river with free flow in Zambia partly due to strong campaigns against its alteration by conservationists (WWF, 2019).

Considering that Zambia is large with several orographic variations, we noted that spatial averages at the country level could potentially obscure maximum WPDs across some regions. We, therefore, further analysed temporal WPD changes across central (Lon 27°–29°E and Lat 17°–14°S) and northern (Lon 30°–33°E and Lat 11°–9°S) Zambia, the two parts of the country showing higher WPDs. Results indicate that while the projected annual average WPD across the whole country is 46.6 $W \cdot m^{-2}$, across central Zambia it is expected to average 63.2 and 56.3 $W \cdot m^{-2}$ over northern Zambia. Two trends emerge, on average, Zambia is expected to experience minor WPD increments of 0.004 $W \cdot m^{-2}$ per year from 2031 to 2050 while slightly larger increments of 0.09 $W \cdot m^{-2}$ per year are to be expected across northern Zambia. On the other hand, central Zambia, the country's region with the highest WPD will potentially experience reductions of ~0.04 $W \cdot m^{-2}$ per year (Figure 11).

4 | CONCLUDING REMARKS

Studies investigating wind speed variations are crucial to the planning of wind energy investments around the world. While causal factors of wind speed variations are well understood, little is known about the spatiotemporal patterns across southern Africa, particularly in Zambia. Therefore, we examined wind speed and wind power potential across Zambia. The findings reported here shed new light on long-term changes (1979–2100) in wind power potential across the country. The most striking result from this study is that at an average of 2.8 $m \cdot s^{-1}$, wind speed is very slow, it is increasing but remains unlikely to support large commercial wind farms that require wind power densities (WPDs) of >200 $W \cdot m^{-2}$. At the observed and projected maximum of ~80 $W \cdot m^{-2}$, small-scale wind turbines and farm-level irrigation projects seem more suitable for the Zambian case.

ACKNOWLEDGEMENTS

This work was financially supported by the Alexander von Humboldt (AvH) Foundation, the foundation is hereby acknowledged. It should be noted however that the AvH Foundation was not involved in the conception, analytical design, data analyses, interpretation of the data, manuscript writing, or the decision to submit this work for publication. The Editor and reviewers are also appreciated for their comments that further helped to improve this work. Open Access funding enabled and organized by Projekt DEAL.

CONFLICT OF INTEREST

The authors declare no potential conflict of interest.

ORCID

Brigadier Libanda https://orcid.org/0000-0001-8215-5572
Heiko Paeth https://orcid.org/0000-0001-8145-4706

REFERENCES

Abatzoglou, J., Dobrowski, S., Parks, S. and Hegewisch, K. (2018) TerraClimate, a high-resolution global dataset of monthly climate and climatic water balance from 1958–2015. *Scientific Data*, 5(1), 170191. https://doi.org/10.1038/sdata.2017.191.

Abdi, O. (2019) Climate-triggered insect defoliators and forest fires using multitemporal Landsat and TerraClimate data in NE Iran: an application of GEOBIA TreeNet and panel data analysis. *Sensors*, 19(18), 3965. https://doi.org/10.3390/s19183965.

Akinsanola, A., Ogunjobi, K., Abolude, A. and Salack, S. (2021) Projected changes in wind speed and wind energy potential over West Africa in CMIP6 models. *Environmental Research Letters*, 16(4), 044033. https://doi.org/10.1088/1748-9326/abed7a.

Akinsanola, A.A., Ogunjobi, K.O., Abolude, A.T., Sarris, S.C. and Ladipo, K.O. (2017) Assessment of wind energy potential for small communities in south-south Nigeria: case study of Koluama, Bayelsa state. *Journal of Fundamentals of Renewable Energy and Applications*, 7, 1–6.

Band, S.S., Bateni, S.M., Almazroui, M., Sajjadi, S., Chau, K. and Mosavi, A. (2021) Evaluating the potential of offshore wind energy in the Gulf of Oman using the MENA-CORDEX wind speed data simulations. *Engineering Applications of Computational Fluid Mechanics*, 15(1), 613–626. https://doi.org/10.1080/19942060.2021.1893225.

Brown, B.G., Katz, R.W. and Murphy, A.H. (1984) Time series models to simulate and forecast wind speed and wind power. *Journal of Climate and Applied Meteorology*, 23(8), 1184–1195.

CoC. (2022) *How much wind is needed for a small wind turbine?*. Available at: https://www.calgary.ca/cs/cpb/operations-workplace-centre/bearspaw-owc/wind-need-for-small-turbine.html [Accessed on 11th May 2022].

Czernecki, B., Głogowski, A. and Nowosad, J. (2020) Climate: an R package to access free in-situ meteorological and hydrological datasets for environmental assessment. *Sustainability*, 2020(12), 394. https://doi.org/10.3390/su12010394.

Davy, R., Gnatiuk, N., Pettersson, L. and Bobylev, L. (2018) Climate change impacts on wind energy potential in the European domain with a focus on the Black Sea. *Renewable and Sustainable Energy Reviews*, 81, 1652–1659. https://doi.org/10.1016/j.rser.2017.05.253.

Del Genio, A.D. (1997) Atmosphere. In: Shirley J.H. and Fairbridge, R.W. (Eds.) *Encyclopedia of Planetary Sciences*, pp. 51–54. Chapman & Hall.

Ebita, A., Kobayashi, S., Ota, Y., Moriya, M., Kumabe, R., Onogi, K., Harada, Y., Yasui, S., Miyaoka, K., Takahashi, K., Kamahori, H., Kobayashi, C., Endo, H., Soma, M., Oikawa, Y. and Ishimizu, T. (2011) The Japanese 55-year Reanalysis "JRA-55": an Interim report. *SOLA*, 7, 149–152. https://doi.org/10.2151/sola.2011-038.

El Khchine, Y., Sriti, M. and El Kadri Elyamani, N. (2019) Evaluation of wind energy potential and trends in Morocco. *Heliyon*, 5(6), e01830. https://doi.org/10.1016/j.heliyon.2019.e01830.

Emeksiz, C. and Cetin, T. (2019) In case study: investigation of tower shadow disturbance and wind shear variations effects on energy production, wind speed and power characteristics. *Sustainable Energy Technologies and Assessments*, 35, 148–159. https://doi.org/10.1016/j.seta.2019.07.004.

Fick, S.E. and Hijmans, R.J. (2017) WorldClim 2: new 1 km spatial resolution climate surfaces for global land areas. *International Journal of Climatology*, 37(12), 4302–4315.

Freychet, N., Hegerl, G., Mitchell, D. and Collins, M. (2021) Future changes in the frequency of temperature extremes may be underestimated in tropical and subtropical regions. *Communications Earth & Environment*, 2(1), 1–8. https://doi.org/10.1038/s43247-021-00094-x.

Ginzky, H., Herrmann, F., Kartschall, K., Leujak, W. and Lipsius, K. (2011) *Geoengineering: effective climate protection or megalomania? Methods – statutory framework – environment policy demands*. Available at: https://www.umweltbundesamt.de/sites/default/files/medien/publikation/long/4177.pdf [Accessed on 15th January 2021].

Giorgi, F., Jones, C. and Asrar, G.R. (2009) Addressing climate information needs at the regional level: the CORDEX framework. *World Meteorological Organization Bulletin*, 58(3), 175–183.

Gupta, H.V., Sorooshian, S. and Yapo, P.O. (1999) Status of automatic calibration for hydrologic models: comparison with multilevel expert calibration. *Journal of Hydrologic Engineering*, 4, 135–143.

Haanyika, C. (2008) Rural electrification in Zambia: a policy and institutional analysis. *Energy Policy*, 36(3), 1044–1058. https://doi.org/10.1016/j.enpol.2007.10.031.

Haberyan, K.A. (2018) A >22,000 yr diatom record from the plateau of Zambia. *Quaternary Research*, 89, 33–42. https://doi.org/10.1017/qua.2017.31.

Hachigonta, S. and Reason, C. (2006) Interannual variability in dry and wet spell characteristics over Zambia. *Climate Research*, 32, 49–62. https://doi.org/10.3354/cr032049.

Hafner, M., Tagliapietra, S. and de Strasser, L. (2018) The challenge of energy access in Africa. In: *Energy in Africa. Springer Briefs in Energy*. Cham: Springer. https://doi.org/10.1007/978-3-319-92219-5_1.

Hamed, K.H. and Rao, A.R. (1998) A modified Mann–Kendall trend test for autocorrelated data. *Journal of Hydrology*, 204(1–4), 182–196. https://doi.org/10.1016/S0022-1694(97)00125-X.

Harris, I., Jones, P.D., Osborn, T.J. and Lister, D.H. (2014) Updated high-resolution grids of monthly climatic observations—the CRU TS3.10 dataset. *International Journal of Climatology*, 34, 623–642. https://doi.org/10.1002/joc.3711.

Hennessey, J.P., Jr. (1977) Some aspects of wind power statistics. *Journal of Applied Meteorology*, 16(2), 119–128.

Hersbach, H., Bell, B., Berrisford, P., Hirahara, S., Horányi, A., Muñoz-Sabater, J., Nicolas, J., Peubey, C., Radu, R., Schepers, D., Simmons, A., Soci, C., Abdalla, S., Abellan, X., Balsamo, G., Bechtold, P., Biavati, G., Bidlot, J., Bonavita, M., Chiara, G., Dahlgren, P., Dee, D., Diamantakis, M., Dragani, R., Flemming, J., Forbes, R., Fuentes, M., Geer, A., Haimberger, L., Healy, S., Hogan, R.J., Hólm, E., Janisková, M., Keeley, S., Laloyaux, P., Lopez, P., Lupu, C., Radnoti, G., Rosnay, P., Rozum, I., Vamborg, F., Villaume, S. and Thépaut, J.N. (2020) The ERA5 global reanalysis. *Quarterly Journal of the Royal Meteorological Society*, 146(730), 1999–2049. https://doi.org/10.1002/qj.3803.

Ines, A.V.M. and Hansen, J.W. (2006) Bias correction of daily GCM rainfall for crop simulation studies. *Agricultural and Forest Meteorology*, 138, 44–53. https://doi.org/10.1016/j.agrformet.2006.03.009.

International Renewable Energy Agency. (2017) *Renewable energy: a key climate solution*. Available at: https://www.irena.org/climatechange/Renewable-Energy-Key-climate-solution#:~:text=Renewable%20power%20could%20cover%20up,helping%20to%20mitigate%20climate%20change.&text=With%20this%20increasingly%20favourable%20cost,sense%20in%20purely%20economic%20terms [Accessed on 16th January 2021].

Jánosi, I., Medjdoub, K. and Vincze, M. (2021) Combined wind-solar electricity production potential over north-western Africa. *Renewable and Sustainable Energy Reviews*, 151, 111558. https://doi.org/10.1016/j.rser.2021.111558.

Jung, C. and Schindler, D. (2021) The role of the power law exponent in wind energy assessment: a global analysis. *International Journal of Energy Research*, 45, 8484–8496.

Jung, C. and Schindler, D. (2022) On the influence of wind speed model resolution on the global technical wind energy potential. *Renewable and Sustainable Energy Reviews*, 156, 112001. https://doi.org/10.1016/j.rser.2021.112001.

Kanno, H., Sakurai, T., Shinjo, H., Miyazaki, H., Ishimoto, Y. and Saeki, T. (2013) Indigenous climate information and modern meteorological records in Sinazongwe District, Southern Province, Zambia. *Japan Agricultural Research Quarterly*, 47(2), 191–201. https://doi.org/10.6090/jarq.47.191.

Kikumoto, R.H., Ooka, H. and Sugawara, J. (2017) Observational study of power law approximation of wind profiles within an urban boundary layer for various wind conditions. *Journal of Wind Engineering and Industrial Aerodynamics*, 164, 13–21.

Kubik, M., Coker, P., Barlow, J. and Hunt, C. (2013) A study into the accuracy of using meteorological wind data to estimate turbine generation output. Renew. *Energy*, 51, 153–158.

Li, D., Feng, J., Dosio, A., Qi, J., Xu, Z. and Yin, B. (2020) Historical evaluation and future projections of 100-m wind energy potentials over CORDEX-East Asia. *Journal of Geophysical Research: Atmospheres*, 125, e2020JD032874. https://doi.org/10.1029/2020JD032874.

Liu, F., Sun, F., Liu, W., Wang, T., Wang, H., Wang, X. and Lim, W. (2019) On wind speed pattern and energy potential in China. *Applied Energy*, 236, 867–876. https://doi.org/10.1016/j.apenergy.2018.12.056.

Lovino, M.A., Müller, O.V., Berbery, E.H. and Müller, G.V. (2018) Evaluation of CMIP5 retrospective simulations of temperature and precipitation in northeastern Argentina. *International Journal of Climatology*, 38, e1158–e1175.

Matthew, O. and Ohunakin, O. (2022) Simulating the effects of climate change and afforestation on wind power potential in Nigeria. *Sustainable Energy Technologies and Assessments*, 22, 41–54. https://doi.org/10.1016/j.seta.2017.05.009.

Moemken, J., Reyers, M., Feldmann, H. and Pinto, J.G. (2018) Future changes of wind speed and wind energy potentials in EURO-CORDEX ensemble simulations. *Journal of Geophysical Research: Atmospheres*, 123, 6373–6389. https://doi.org/10.1029/2018JD028473.

Moriasi, D.N., Arnold, M.W., Bingner, R.L., Harmel, R.D. and Veith, T. L. (2007) Model evaluation guidelines for systematic quantification of accuracy in watershed simulations. *Transactions of the ASABE*, 50(3), 885–900. https://doi.org/10.13031/2013.23153.

Munyeme, G. and Jain, P.C. (1994) Energy scenario of Zambia: prospects and constraints in the use of renewable energy resources. *Renewable Energy*, 5, 1363–1370.

Najac, J., Lac, C. and Terray, L. (2011) Impact of climate change on surface winds in France using a statistical-dynamical downscaling method with mesoscale modelling. *International Journal of Climatology*, 31(3), 415–430. https://doi.org/10.1002/joc.2075.

Ngongondo, C., Xu, C., Tallaksen, L. and Alemaw, B. (2012) Evaluation of the FAO Penman–Montheith, Priestley–Taylor and Hargreaves models for estimating reference evapotranspiration in southern Malawi. *Hydrology Research*, 44(4), 706–722. https://doi.org/10.2166/nh.2012.224.

Ogunjobi, K.O., Ajayi, V.O., Folorunsho, A.H. and Iiori, O.W. (2022) Projected changes in wind energy potential using CORDEX ensemble simulation over West Africa. *Meteorology and Atmospheric Physics*, 134(3), 48. https://doi.org/10.1007/s00703-022-00880-y.

Oyedepo, S.O., Adaramola, M.S. and Paul, S.S. (2012) Analysis of wind speed data and wind energy potential in three selected locations in south-east Nigeria. *International Journal of Energy and Environmental Engineering*, 3, 7–9. https://doi.org/10.1186/2251-6832-3-7.

Penar, P. (2016) *What lies behind Africa's lack of access and unreliable power supplies*. Available at: https://theconversation.com/what-lies-behind-africas-lack-of-access-and-unreliable-power-supplies-56521 [Accessed on 4th May 2022].

R Core Team. (2020) *R: A Language and Environment for Statistical Computing*. Vienna, Austria: R Foundation for Statistical Computing.

Ramudu, V. and Alla, M. (2018) Design and analysis of wind turbine by using polymer nano composite materials. *Journal of Emerging Technologies and Innovative Research*, 5(2), 586–590.

Randall, D.A., Wood, R.A., Bony, S., Colman, R., Fichefet, T., Fyfe, J., Kattsov, V., Pitman, A., Shukla, J., Srinivasan, J., Stouffer, R.J., Sumi, A. and Taylor, K.E. (2007) Cilmate models and their evaluation. In: Solomon, S., Qin, D., Manning, M., Chen, Z., Marquis, M., Averyt, K.B., Tignor, M. and Miller, H. L. (Eds.) *Climate Change 2007: The Physical Science Basis. Contribution of Working Group I to the Fourth Assessment Report of the Intergovernmental Panel on Climate Change*. Cambridge and New York, NY: Cambridge University Press.

Reyers, M., Moemken, J. and Pinto, J.G. (2016) Future changes of wind energy potentials over Europe in a large CMIP5 multi-model ensemble. *International Journal of Climatology*, 36(2), 783–796.

Reyers, M., Pinto, J. and Moemken, J. (2014) Statistical-dynamical downscaling for wind energy potentials: evaluation and applications to decadal hindcasts and climate change projections. *International Journal of Climatology*, 35(2), 229–244. https://doi.org/10.1002/joc.3975.

Riahi, K., Rao, S., Krey, V., Cho, C., Chirkov, V., Fischer, G., Kindermann, G., Nakicenovic, N. and Rafaj, P. (2011) RCP 8.5—a scenario of comparatively high greenhouse gas emissions. *Climatic Change*, 109, 33–57. https://doi.org/10.1007/s10584-011-0149-y.

Rosenbloom, D., Markard, J., Geels, F. and Fuenfschilling, L. (2020) Why carbon pricing is not sufficient to mitigate climate change—and how "sustainability transition policy" can help. *Proceedings of the National Academy of Sciences of the United States of America*, 117(16), 8664–8668. https://doi.org/10.1073/pnas.2004093117.

Rueda, F.J., Schladow, S.G. and Monismith, S.G. (2005) On the effects of topography on wind and the generation of currents in

a large multi-basin lake. *Hydrobiologia*, 532, 139–151. https://doi.org/10.1007/s10750-004-9522-4.

Sarkodie, S. and Adams, S. (2020) Electricity access and income inequality in South Africa: evidence from Bayesian and NARDL analyses. *Energy Strategy Reviews*, 29, 100480. https://doi.org/10.1016/j.esr.2020.100480.

Sawadogo, W., Abiodun, B.J. and Okogbue, E.C. (2019) Projected changes in wind energy potential over West Africa under the global warming of 1.5°C and above. *Theoretical and Applied Climatology*, 138, 321–333.

Schaeffer, R., Szklo, A.S., Pereira de Lucena, A.F., Borba, M.C., Pupo Nogueira, L.P., Fleming, F.P., Troccoli, A., Harrison, M. and Boulahya, M.S. (2012) Energy sector vulnerability to climate change: a review. *Energy*, 38(1), 1–12. https://doi.org/10.1016/j.energy.2011.11.056.

Schulzweida, U. (2021) *CDO user guide (version 2.0.0)*. Zenodo. https://doi.org/10.5281/zenodo.5614769.

Shonhiwa, C. (2015) An assessment of wind power generation potential for Margate town in South Africa. *International Journal of Energy and Power Engineering*, 4(2), 32. https://doi.org/10.11648/j.ijepe.20150402.13.

Shrestha, M. (2015) Data analysis relied on linear scaling bias correction (V.1.0) Microsoft Excel file.

Shrestha, M., Acharya, S. and Shrestha, P. (2017) Bias correction of climate models for hydrological modelling—Are simple methods still useful? *Meteorological Applications*, 24(3), 531–539. https://doi.org/10.1002/met.1655.

Sillmann, J., Kharin, V.V., Zwiers, F.W., Zhang, X. and Bronaugh, D. (2013) Climate extremes indices in the CMIP5 multimodel ensemble. Part 2: future climate projections. *Journal of Geophysical Research: Atmospheres*, 118, 2473–2493.

Storm, B., Dudhia, J., Basu, S., Swift, A. and Giammanco, I. (2009) Evaluation of the weather research and forecasting model on forecasting low-level jets: implications for wind energy. *Wind Energy*, 12, 81–90.

Taylor, K.E. (2001) Summarizing multiple aspects of model performance in a single diagram. *Journal of Geophysical Research*, 106, 7183–7192.

Teutschbein, C. and Seibert, J. (2012) Bias correction of regional climate model simulations for hydrological climate-change impact studies: review and evaluation of different methods. *Journal of Hydrology*, 456–457, 12–29.

Thomson, A.M., Calvin, K.V., Smith, S.J., Kyle, G.P., Volke, A., Patel, P., Delgado-Arias, S., Bond-Lamberty, B., Wise, M.A., Clarke, L.E. and Edmonds, J.A. (2011) RCP4.5: a pathway for stabilization of radiative forcing by 2100. *Climatic Change*, 109, 77–94. https://doi.org/10.1007/s10584-011-0151-4.

Tse, K., Weerasuriya, A. and Hu, G. (2020) Integrating topography-modified wind flows into structural and environmental wind engineering applications. *Journal of Wind Engineering and Industrial Aerodynamics*, 204, 104270. https://doi.org/10.1016/j.jweia.2020.104270.

Türk, M. and Emeis, S. (2010) The dependence of offshore turbulence intensity on wind speed. *Journal of Wind Engineering and Industrial Aerodynamics*, 98(8–9), 466–471. https://doi.org/10.1016/j.jweia.2010.02.005.

Turner, J. (1999) A realizable renewable energy future. *Science*, 285(5428), 687–689. https://doi.org/10.1126/science.285.5428.687.

UNFPA. (2010) *Population trends*. Available at: https://esaro.unfpa.org/en/topics/population-trends#:~:text=In%202010%2C%20the%20estimated%20population,870%20million%20in%20Eastern%20Africa [Accesssed on 16th January 2021].

Wagner, J., Gohm, A. and Rotach, M. (2014) The impact of valley geometry on daytime thermally driven flows and vertical transport processes. *Quarterly Journal of the Royal Meteorological Society*, 141(690), 1780–1794. https://doi.org/10.1002/qj.2481.

Weber, J., Wohland, J., Reyers, M., Moemken, J., Hoppe, C., Pinto, J.G. and Witthaut, D. (2018) Impact of climate change on backup energy and storage needs in wind-dominated power systems in Europe. *PLoS ONE*, 13, e0201457. https://doi.org/10.1371/journal.pone.0201457.

WMO. (2013) *Guide to the Global Observing System*. Geneva: WMO. WMO No. 488. Available at: https://community.wmo.int/wmo-no-488-guide-global-observing-system [Accessed on 5th June, 2022].

WMO. (2017) *WMO Guidelines on the Calculation of Climate Normals*. Geneva: WMO. WMO No. 1203. Available at: https://library.wmo.int/doc_num.php?explnum_id=4166 [Accessed on 31st May 2022].

Wood, D. (2011) Small wind turbines. In: Sathyajith, M. and Philip, G. (Eds.) *Advances in Wind Energy Conversion Technology*. *Environmental Science and Engineering*. Berlin-Heidelberg: Springer. https://doi.org/10.1007/978-3-540-88258-9_8.

World Bank. (2019) *Electricity Access in Sub-Saharan Africa Uptake, Reliability, and Complementary Factors for Economic Impact*. Washington, DC: World Bank. Available at: https://openknowledge.worldbank.org/bitstream/handle/10986/31333/9781464813610.pdf [Accessed on 4th May 2022].

Wright, M. and Grab, S. (2017) Wind speed characteristics and implications for wind power generation: cape regions, South Africa. *South African Journal of Science*, 113, 7–8. https://doi.org/10.17159/sajs.2017/20160270.

WWF. (2019) *Zambia halts hydropower dam on Luangwa River*. Available at: https://wwf.panda.org/wwf_news/?349071/Zambia-halts-hydropower-dam-on-Luangwa-river [Accessed on 11th May 2022].

Zaharim, A., Najid, S., Razali, M. and Sopian, K. (2008) The suitability of statistical distribution in fitting wind speed data. *WSEAS Transactions on Mathematics*, 7, 12.

Zeng, Z., Ziegler, A., Searchinger, T., Yang, L., Chen, A., Ju, K., Piao, S., Li, L.Z.X., Ciais, P., Chen, D., Liu, J., Azorin-Molina, C., Chappell, A. and Medvigy, D. (2019) A reversal in global terrestrial stilling and its implications for wind energy production. *Nature Climate Change*, 9(12), 979–985. https://doi.org/10.1038/s41558-019-0622-6.

Zhou, J., Zhao, X., Wu, J., Huang, J., Qiu, D., Xue, D., Li, Q., Liu, C., Wei, W., Zhang, D. and Yang, X. (2021) Wind speed changes and influencing factors in inland river basin of monsoon marginal zone. *Ecological Indicators*, 130, 108089. https://doi.org/10.1016/j.ecolind.2021.108089.

How to cite this article: Libanda, B., & Paeth, H. (2023). Modelling wind speed across Zambia: Implications for wind energy. *International Journal of Climatology*, *43*(2), 772–786. https://doi.org/10.1002/joc.7826